J. Fluid Mech. (1996), *vol.* 316, *pp.* 139–161

A random-flight evaluation of the constants of relative dispersion in idealized turbulence

By ALAN J. FALLER
78 Bellevue Ave., Melrose, MA 02176, USA

(Received 25 May 1995 and in revised form 4 December 1995)

In the idealized problem of homogeneous isotropic stationary inertial-range turbulence the rate of relative dispersion of an ensemble of tracer pairs can be characterized by a constant C_0. In order to compute this constant with random-flight equations, however, it is necessary first to know the values of two other constants, C_1 and C_2, that occur in the two-particle velocity-component relations of Lagrangian tracers (Faller 1992).

C_1 and C_2 are found by an elaborate trial and error procedure in a new two-tracer random-flight model of dispersion that matches input and output values of these two variates. The constant C_0 is then computed using the Lagrangian relations and is found to be significantly smaller than when the Eulerian Kármán/Howarth correlations are used.

The probability density distribution of tracer separations has a kurtosis slightly larger than that of a comparable Gaussian distribution. At small spacings the frequency of tracer spacings is six to ten times larger than would be expected from a Gaussian distribution. The distribution function for the speed of separation of the Lagrangian tracers has a negative skewness similar to that found for two-point Eulerian velocities.

1. Introduction

The concept of relative dispersion was introduced by L. F. Richardson (1926) who considered the expansion of puffs of tracers of different spatial scales in the turbulent atmosphere. The following is a brief summary of some of his conclusions. Richardson noted that scales of turbulence much larger than the characteristic diameter of a puff, d, would simply convect the puff; scales of turbulence much smaller than d would act as Fickian diffusion; but scales of turbulence close to d would expand the puff by tearing it apart in an irregular manner that would be impossible to describe in any individual case. He noted that it was necessary to consider the dispersion of a large ensemble of superimposed puffs, each taken relative to its centre of mass. We may call such an ensemble of puffs a 'cloud', and in isotropic turbulence such a cloud will expand symmetrically about its centre.

Richardson further deduced that the rate of expansion of the mean-square radius of tracers in a single puff, $\tilde{\rho}^2$, could be represented by the mean-square distance between all possible pairs of tracers in the puff: $\tilde{r}^2 = 2\tilde{\rho}^2$. Moreover, he noted that the growth of $\tilde{r}^2$ for the cloud could be obtained from many randomly selected pairs of tracers, e.g. one pair representing each puff.

This study is concerned with 'idealized' (homogeneous isotropic stationary inertial-range) three-dimensional relative turbulent dispersion. Its purposes are: (i) to provide estimates of the characteristics of relative dispersion until the day when full-scale numerical simulations or observations can provide more exact information; and (ii) to

provide a method for the rapid computation of dispersion that, hopefully, can be extended to more-realistic turbulent dispersion situations. These goals are attained in part in a new 'random-flight' (Durbin 1980) model which integrates the evolution of the spacings of many thousands of pairs of tracers, a Monte-Carlo approach with each pair calculated separately.

The major goals of the model are the determination of: (i) the constants C_1 and C_2 that characterize the difference between the two-point Eulerian correlations of velocity components and the corresponding two-tracer Lagrangian relations (Faller 1992); (ii) the constant C_0 that measures the rate of dispersion; (iii) the probability density distribution of tracer separations, related to the concentration of pollutants; and (iv) the correlation timescale for the separation of tracers.

To find C_0 and other characteristics of relative dispersion it is first necessary to simultaneously evaluate and find 'consistent' values of C_1 and C_2, i.e. matched input and output values found by trial and error. These coefficients should be found from Lagrangian statistics, i.e. along trajectories, which are unavailable in advance of the solution, so this is essentially a 'bootstrap' operation.

The random-flight approach is straightforward and computationally efficient. The basic random-flight equation is also described as a Langevin equation, a correlated random-walk, a first-order Markov process and an Uhlenbeck–Ornstein procedure. Single-tracer applications have already demonstrated the utility of the method in a variety of practical applications (e.g. Durbin 1980; Thomson 1986; van Dop & Nieuwstadt 1985; Faller & Auer 1988). While there have been several attempts to validate this approach (e.g. Durbin 1983; Thomson 1987) a complete theoretical justification of even the single-tracer problem remains elusive. Nevertheless as shown in Faller & Auer (1988), for single tracers the dispersion is found to exactly match the theoretical prediction of Taylor (1921) at large times when a proper definition of the time step is used. Thus it seems that the random–flight equation provides suitable kinematics while the dynamics is statistically represented by specification of the mean-square turbulent velocity, $[u'^2]$, and the Lagrangian integral timescale, T, both of which also must be specified to evaluate Taylor's equation.

Two-tracer models are fundamentally different, however, and at the very least should satisfy the two-tracer kinematic relations of turbulence. For a review of earlier two-tracer models and their application to concentration distributions one may refer to Thomson (1990) and to Borgas & Sawford (1994). The latter authors used Thomson's approach and were concerned about deficiencies in that model and a lack of uniqueness. The present model differs in several ways. First, whereas previous modellers have based their method on Eulerian velocity correlations, here the two-tracer second-order relations for Lagrangian tracers, as derived in Faller (1992), are directly satisfied. Secondly, the unmodified random-flight equations are used for each tracer and thus they satisfy Taylor's (1921) single-particle diffusion results. Thirdly, apart from the two approximations noted in Faller (1992) (and use of the random-flight equations) there are no further approximations. Finally, the solution is unique (apart from stochastic uncertainty) and internally consistent.

In three-dimensional turbulence we have the familiar inertial subrange with the slope $S = -5/3$ when the logarithm of the energy density ($\ln E$) is plotted against the logarithm of the wave number ($\ln k$). Possible slight departures from this idealized slope will not be considered here, but one can conceive of other values of S and ask about the characteristics of dispersion in such cases. This model can easily handle cases other than $S = -5/3$ (Faller & Choi 1985) if such studies are warranted.

2. Terminology and notation

For the inertial subrange it is required that the non-dimensional tracer separation satisfy $r = r'/L \ll 1$ where L is the Eulerian integral lengthscale of the turbulence and primes denote dimensional variates. Viscous effects are omitted with the assertion that all r' are much larger than the Kolmogorov microscale. There are assumed to be a Lagrangian timescale, T, and a root mean square (r.m.s.) component speed, $u' = [(u_i' u_i')/3]^{1/2} = 1, i = 1\text{–}3$. These parameters are related by

$$Cs = L/u'T, \tag{1}$$

where Cs has been called the Corrsin constant (Faller 1992) and, following Corrsin (1963) and Tennekes & Lumley (1972), for three-dimensional turbulence $Cs \approx 3$. Cs is a free parameter of this model, but it will emerge that the non-dimensional results are independent of Cs over a reasonable range of possible values. Velocities, lengths, and times are made dimensionless by u', L, and L/u', respectively. Thus for the components of u' and the components of r' the non-dimensional variates are $u_i = u_i'/u'$ and $r_i = r_i'/L$, and non-dimensional time is $t = t'u'/L = t'/(CsT)$. It is important to recognize that in these computations the cloud of tracers always remains in the inertial subrange with $r \ll 1$ and with $t \ll 1$.

The vector $\boldsymbol{r}$ extends from point 1 to point 2 (figure 1) which have velocities $\boldsymbol{u}_1$ and $\boldsymbol{u}_2$. The velocity components in an arbitrary rectangular coordinate system are $u_{1,i}$ and $u_{2,i}$, and the components parallel to and normal to $\boldsymbol{r}$ are $u_{1,p}$, $u_{2,p}$, $u_{1,n}$ and $u_{2,n}$.

Three special ensemble averages are used:

E1: averages indicated by a tilde. All tracer pairs have travelled for a specified elapsed time, t_S, from some distribution of initial spacings, $\boldsymbol{r}_o$. Many different lengths and orientations of the $\boldsymbol{r}$ at time t_S are included in this ensemble in contrast to ensembles E2 and E3.

E2: averages indicated by angular brackets. All tracer pairs have the same specified length, r_S, at some fixed time, t_f, and all orientations of $\boldsymbol{r}$ are included.

In a cloud of tracers observations of all tracer-pair spacings at some t_f could be assigned to many intervals $r_n \pm \Delta r$ and E2-averages of some function of r would be found for each r_n. For time-independent turbulence the data from many specified times could be combined for each r_n. In this way averages $\langle U \rangle (r_n)$ and $\langle U^2 \rangle (r_n)$ for the calculation of $C_1(r_n)$ and $C_2(r_n)$ from (3) and (4) (below) could be found.

In the present model tracer pairs are integrated separately from some distribution of initial values, r_o, and the value of r when some tracer reached t_f could be classified into $r_n \pm \Delta r$ as above. But because C_1 and C_2 are constant in the inertial subrange, a more efficient method than the direct use of (3) and (4) has been used for the evaluation of these constants, as discussed in §6.2.

E3: averages indicated by an overbar. These are similar to an E2 average but all tracer pairs have the same specified vector, $\boldsymbol{r}_S$, as in the development of the Kármán/Howarth relations (Kármán & Howarth, 1938; also see Batchelor, 1953).

Averages other than E1, E2 or E3 will be denoted by square brackets.

The general rate of expansion of a cloud of tracers is represented by the constant C_0 in the formula

$$\mathrm{d}r^+/\mathrm{d}t = C_0 (r^+)^\beta, \tag{2}$$

where $r^+ = (\tilde{r}^2)^{1/2}$ is the r.m.s. r in E1, and, as shown by several authors, $\beta = 1/3$ for three-dimensional idealized turbulence. In Appendix A dimensional arguments show that the relation $\beta = -(S+1)/2$ may have more general applicability.

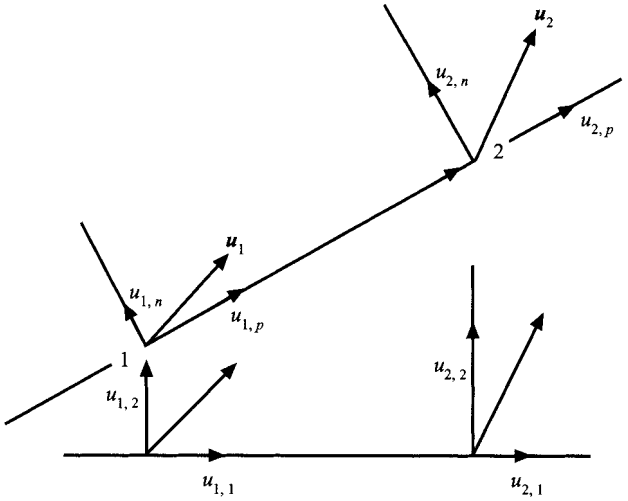

FIGURE 1. The vector r between points 1 and 2 and components of the velocities u_1 and u_2 in two dimensions.

The average rate of expansion of all tracer pairs having the same spacing r_S defines C_1 by

$$\langle U \rangle = \langle \mathrm{d}r/\mathrm{d}t \rangle = C_1 r_S^{\beta} \tag{3}$$

where $U = u_{2,p} - u_{1,p}$ is the rate of separation of an individual pair of tracers. C_2 is defined similarly but is based upon the r.m.s. expansion speed and is given by

$$\langle U^2 \rangle^{1/2} = \langle (\mathrm{d}t/\mathrm{d}t)^2 \rangle^{1/2} = C_2 r_S^{\beta}. \tag{4}$$

The relation between C_1 and C_2 is simply

$$\Sigma(r_S) = \langle U^2 \rangle - \langle U \rangle^2 = (C_2^2 - C_1^2)(r_S)^{2\beta}, \tag{5}$$

where Σ is the variance of U in E2.

In statistical summaries 'Gaussian' refers to any distribution of the form $A(\exp(-(x-x)^2))$, where A is a factor related to the area under the curve, whereas 'normal' refers to a Gaussian with zero mean and unit sd. If the components x_i of some vector x have Gaussian forms with zero mean, then the length x has a distribution of the form $B(x^2 \exp(-x^2))$ where B is some factor, and this will be referred to as a three-dimensional Gaussian.

3. The random-flight procedure

A recursion relation for the velocity components of a single tracer is taken to be

$$u_{i,m} = Ru_{i,m-1} + Q\hat{u}_{i,m}, \quad Q = (1-R^2)^{1/2}, \quad i = 1\text{–}3, \tag{6}$$

where m is the time-step index, $\hat{u}_{i,m}$ is a random contribution to $u_{i,m}$, and R is the one-time-step autocorrelation of u_i. Equation (6) is a random-flight model equation that represents the effects of the turbulence on the velocity of a single parcel of fluid in place of the full dynamic equations of motion. At any time step each component is presumed to have a persistence, represented by the term $Ru_{i,m-1}$, and a random impulse from other fluid parcels, represented by $Q\hat{u}_{i,m}$.

When a forward time step is used to convect a tracer, specifically

$$x_{i,m+1} = x_{i,m} + u_{i,m}\,\Delta t, \tag{7}$$

then R is related to the time step $\Delta t'$ and to T by

$$R = (2-\Delta t'/T)/(2+\Delta t'/T) = (2-Cs\Delta t)/(2+Cs\Delta t) \tag{8}$$

which can be used in single-particle dispersion problems with $\Delta t'$ up to $2T$ when $t' \gg T$ (Faller & Auer 1988). The case $\Delta t' = 2T$ ($R = 0, Q = 1$) is a random walk, and a corollary is that a random walk with step $\Delta t'$ implies an integral scale $T = \Delta t'/2$. The more commonly used expression $R = \exp(-\Delta t'/T)$ is a second-order approximation to (8).

The use of (6) guarantees that u_i will have a normal distribution if the $\hat{u}_i$ are drawn from a normal population. If the $\hat{u}_i$ come from some other population, say of a top-hat form, the distribution of u_i will be a function of R, approaching normality as $R \to 1 (\Delta t \to 0)$.

That R is indeed a one-time-step autocorrelation may be seen by multiplying (6) by $u_{i,m-1}$ and averaging over many time steps. Accordingly, (6) gives a stepwise decay of the autocorrelation $[u_{i,m}\,u_{i,m-k}]$ (time lag $k\Delta t$) that is an approximation to a continuous exponential decay of the autocorrelation of u_i.

We now consider the rate of separation of two tracers with vector spacing $\boldsymbol{r}$. A random-flight equation is applied to each tracer, but the velocities of the two tracers will be correlated so that all second-order two-tracer Lagrangian velocity relations are satisfied statistically.

The non-dimensional random-flight equations for two tracers are

$$u_{1,i,m} = R_m\,u_{1,i,m-1} + Q_m\,\hat{u}_{1,i,m}, \tag{9}$$

$$u_{2,j,m} = R_m\,u_{2,j,m-1} + Q_m\,\hat{u}_{2,j,m}, \tag{10}$$

where the subscripts m on R_m and Q_m indicates that these will be changed with time. It is necessary to change Δt, and therefore R and Q, at each time step because the spacing r increases over several orders of magnitude.

The corresponding convection equations are

$$x_{1,i,m+1} = x_{1,i,m} + u_{1,i,m}\,\Delta t_m, \tag{11}$$

$$x_{2,i,m+1} = x_{2,i,m} + u_{2,i,m}\,\Delta t_m, \tag{12}$$

and the component spacings are $r_{i,m} = x_{2,i,m} - x_{1,i,m}$.

Because we are in the inertial subrange of turbulence with scales of motion much larger than r, the velocity components $u_{1,i}$ and $u_{2,j}$ must be spatially related. It follows that the six random contributions, $\hat{u}_{1,i}$ and $\hat{u}_{2,j}$ (the six $\hat{u}$) should be spatially correlated, as well. If they are not it follows that the $u_{1,i}$ and $u_{2,j}$ themselves will gradually become uncorrelated. Thomson (1990) and Borgas & Sawford (1994) used uncorrelated $\hat{u}$ but maintained correlations of the u by applying modified random-flight equations with a more complex Ru term. It is argued here, however, that the $\hat{u}$ represent impulses from all scales of turbulence, and those scales comparable to and larger than r should contribute correlated $\hat{u}$. Of course it would seem on physical grounds that if the $\hat{u}$ have spatial correlation they should also have temporal correlation. Nevertheless, the $\hat{u}$ should be selected here without temporal correlation because this is already specified by R. Thus in this formulation the random-flight equations remain unmodified, the

temporal correlation is retained in the Ru terms, and the spatial correlation enters through the random components.

The $\hat{u}$ are chosen at each time step as each tracer pair is individually integrated. But this must be done in such a way that the required relations between the components of $\boldsymbol{u}_1$ and $\boldsymbol{u}_2$ will be satisfied after the trajectories of many thousands of tracer pairs have been integrated. The detailed procedure for selecting the $\hat{u}$ is given in §5 and Appendix D, but for the present let us assume that a satisfactory method does exist.

In relative dispersion the individual values of $u_{1,i}$, $u_{2,i}$, $x_{1,i}$ and $x_{2,i}$ are of little direct interest since only the differences contribute. Therefore, it is often convenient in the computations to deal with the velocity component differences $U_i = u_{2,i} - u_{1,i}$ and the component spatial differences, $r_i = x_{2,i} - x_{1,i}$. The actual computations, however, use (9) and (10) directly. If the $\hat{u}_{1,i}$ and $\hat{u}_{2,j}$ come from normal distributions then the $u_{1,i}$ and $u_{2,j}$ also will be normally distributed throughout the computations, as should be the case. At the same time the correlations of $\hat{u}_{1,i}$ and $\hat{u}_{2,j}$ provide the correct relations between the $u_{1,i}$ and $u_{2,j}$ which vary with the particle spacing. With this formulation it is not necessary to introduce correction terms similar to those introduced by Thomson (1990) in his somewhat different formulation of the problem.

4. The kinematic constraints

This section summarizes and augments the results of an earlier study (Faller 1992) concerning the difference between two-point Eulerian velocity correlations and two-tracer Lagrangian relations. Consider the parallel components of velocity $u_{1,p}$ and $u_{2,p}$ at two points separated by $\boldsymbol{r}$ (figure 1). For fixed points and for isotropic turbulence $\langle u^*_{1,p}\rangle = \langle u^*_{2,p}\rangle = 0$ where asterisks refer to Eulerian observations or relations. In contrast, for pairs of Lagrangian tracers with a specified spacing, r_S, on average the tracers disperse with $\langle U\rangle = \langle u_{2,p} - u_{1,p}\rangle > 0$, and by symmetry $\langle u_{2,p}\rangle = -\langle u_{1,p}\rangle = \langle U\rangle/2$. These facts should be incorporated into the relations between the velocities of the two tracers in any dispersion model.

The relation $\langle U\rangle > 0$ has frequently been questioned and deserves elaboration. $U = (u_{2,p} - u_{1,p})$ is the projection of $\boldsymbol{U} = (\boldsymbol{u}_2 - \boldsymbol{u}_1)$ on $\boldsymbol{r}$ hence $\langle U\rangle = \langle \boldsymbol{U}\cdot\boldsymbol{r}/r\rangle$. If $\boldsymbol{U}$ and $\boldsymbol{r}$ were independent it would follow that $\langle U\rangle = 0$. But $\boldsymbol{r}$ does not have random orientation with respect to $\boldsymbol{U}$. As shown below, the relation between $\boldsymbol{U}$ and $\boldsymbol{r}$ arises from the persistence of $\boldsymbol{U}$ that is associated with a finite Lagrangian timescale, T.

Consider the change of $\boldsymbol{r}$ with a constant $\boldsymbol{U}$, i.e. with $T \to \infty$. If $U > 0$ it is easily seen that $\boldsymbol{r}$ becomes more parallel to $\boldsymbol{U}$, thus making the product $U = \boldsymbol{U}\cdot\boldsymbol{r}/r$ increase with time. Conversely, for a long-persistent $\boldsymbol{U}$ with $U < 0$, $\boldsymbol{r}$ becomes more perpendicular to $\boldsymbol{U}$, and so U decreases and eventually becomes positive. Clearly, for any finite T each tracer pair tends to have a positive average U, and this is the essence of dispersion. It follows that the selection of many tracer pairs with any fixed r_f will yield $\langle U\rangle > 0$. Even with a random walk (in time) there is an implied $T = \Delta t'/2$ (see text following (8)) that is responsible for random-walk dispersion. Moreover, any dispersion model must result in $\langle U\rangle > 0$ regardless of its formulation.

For isotropic turbulence the second-order Eulerian two-point velocity component correlations can be found from the Kármán/Howarth (1938) relations

$$\mu^*_{i,j} = \overline{u^*_{1,i}u^*_{2,j}} = (f^* - g^*)r_i r_j/r^2 + g^*\delta_{i,j} \quad \text{(E3 average)}, \tag{13}$$

where

$$f^* = \langle u^*_{1,p}u^*_{2,p}\rangle \quad \text{(E2 averages)} \tag{14}$$

and

$$g^* = \langle u^*_{1,n}u^*_{2,n}\rangle. \tag{15}$$

Here $\mu^*_{i,j}$, f^* and g^* are correlation coefficients and subscripts p and n refer to the parallel and normal components relative to $\boldsymbol{r}$.

For a three-dimensional non-divergent fluid

$$g^* = f^* + (r/2)\,\mathrm{d}f^*/\mathrm{d}r \tag{16}$$

leaving f^* as the only variate needed to determine the $\mu^*_{i,j}$. But the development of (16) required the explicit assumption of a non-divergent fluid and is not strictly applicable to diverging Lagrangian tracers. Moreover, although (13) still applies (i.e. without asterisks), f (as opposed to f^*) is not a correlation coefficient because the means $\langle u_{1,p}\rangle$ and $\langle u_{2,p}\rangle$ are not zero and the standard deviations $\sigma(u_{1,p}) = \sigma(u_{2,p}) \neq 1$. Similarly, although $\langle u_{1,n}\rangle = \langle u_{2,n}\rangle = 0$, g is not a correlation coefficient because the standard deviations $\sigma(u_{1,n}) = \sigma(u_{2,n}) \neq 1$ (Appendix B).

The development of expressions for f and g appropriate to diverging tracers as given in Faller (1992) relied on one basic assumption and one approximation: it was asserted that g could be derived from a development similar to that of Kármán & Howarth (1938) but for a divergent fluid, the divergence being given by $D = 3\langle U\rangle/r_S$, the divergence of those tracers at the specified r_S. More precisely, the assumption was that the Eulerian velocity relations for a divergent fluid (having an average particle separation rate $\langle U\rangle = Dr_S/3$) can be substituted for the required Lagrangian relations in a non-divergent fluid (where pairs of tracers with spacing r_S separate at rate $\langle U\rangle$). While this assumption may appear to be reasonable, its full justification (or degree of validity) will require a complete Lagrangian theory or suitable numerical solution of the full dynamic equations.

The approximation needed to find f was that $u^*_{1,p}$, $u^*_{2,p}$, and their difference, U^*, had Gaussian distributions. Although U^* has a known (Monin & Yaglom 1971) and measurable (Anselmet *et al.* 1984) skewness, this enters only into third- and higher-order correlations, and to second order U^* is approximately Gaussian.

From Faller (1992) the equations for the velocity component relations for divergent Lagrangian tracers are then

$$\overline{u_{1,i}\,u_{2,j}} = (f-g)\,r_i r_j/r^2 + g\delta_{i,j}, \tag{17}$$

$$f = \langle u_{1,p}\,u_{2,p}\rangle = (1+f^*)/2 - \langle U^2\rangle/4, \tag{18}$$

$$g = \langle u_{1,n}\,u_{2,n}\rangle = f + (r/2)\,\mathrm{d}f/\mathrm{d}r + (3\langle U\rangle^2)/4. \tag{19}$$

Here $\langle U\rangle$ and $\langle U^2\rangle$ are unknown functions of r, very much complicating the problem. But in the inertial subrange we can substitute (3) and (4) to express (18) and (19) in terms of the (unknown) constants C_1 and C_2. Moreover, in the inertial subrange

$$f^* = \exp(-r^\alpha), \tag{20}$$

where $\alpha = 2/3$ (Dickey & Mellor 1979, and Appendix A). Then, for $r \ll 1$, $f^* = 1 - r^{2/3}$ and (17) reduces to

$$\mu_{i,j,} = \overline{u_{1,i}}\,u_{2,j} = r^{2/3}(\tfrac{1}{6} + C_2^2/12 - 3C_1^2/4)\,r_i r_j/r^2 + (1 + r^{2/3}(-2/3 - C_2^2/3 + 3C_1^2/4))\,\delta_{i,j}. \tag{21}$$

The corresponding Eulerian Kármán/Howarth result is found by setting $C_1 = 0$ and $C_2^2 = 2$ (Appendix B) and is

$$\mu^*_{i,j,} = \overline{u^*_{1,i}\,u^*_{2,j}} = r^{2/3} r_i r_j/3r^2 + (1 - (4/3)r^{2/3})\,\delta_{i,j}. \tag{22}$$

The determination of C_1 and C_2 by trial and error is explained in §§5 and 6, but for the present assume that these constants are known.

By isotropy the matrix $\mu_{i,j}$ is symmetrical with the six independent entries

$$\mu_{i,j} = \begin{pmatrix} \overline{u_{1,1}u_{2,1}} & \overline{u_{1,1}u_{2,2}} & \overline{u_{1,1}u_{2,3}} \\ — & \overline{u_{1,2}u_{2,2}} & \overline{u_{1,2}u_{2,3}} \\ — & — & \overline{u_{1,3}u_{2,3}} \end{pmatrix} \tag{23}$$

and these must be satisfied in the computations. For each tracer pair and at each time step these necessary averages can be found from (21) given C_1, C_2 and $\boldsymbol{r}$.

5. Determination of the random velocity components and the time step

The evolution of each tracer pair is integrated individually and at each time step six $\hat{u}$ must be chosen to implement (9) and (10). The E3-average of the product of (9) and (10) may be written, after rearrangement, as

$$\overline{(\hat{u}_{1,i}\hat{u}_{2,j})}_m = ((\overline{u_{1,i}u_{2,j}})_m - R_m^2(\overline{u_{1,i}u_{2,j}})_{m-1})/Q_m^2 \quad \text{(E3)} \tag{24}$$

or, more concisely,

$$\hat{\mu}_{i,j,m} = (\mu_{i,j,m} - R_m^2\mu_{i,j,m-1})/(1-R_m^2). \tag{25}$$

Here it may be noted that although $\mu_{i,j,m}$ and $\mu_{i,j,m-1}$ are not correlations, $\hat{\mu}_{i,j,m}$ is a correlation because $\hat{u}_{1,i}$ and $\hat{u}_{2,j}$ are drawn from a normal distribution. The determination of individual values of the $\hat{u}$ at each step now requires two distinct procedures: (*a*) an evaluation of the right-hand side of (25), and (*b*) a conversion of the $\hat{\mu}_{i,j,m}$ into individual values of the $\hat{u}$ for use in (9) and (10).

(*a*) Given values of C_1, C_2, and $\boldsymbol{r}$, the $\mu_{i,j,m}$ in (25) are readily found from (21). But evaluation of the $\mu_{i,j,m-1}$ is not as obvious. Note in particular that this term is a statistic and cannot be computed from the values $u_{1,i,m-1}$ and $u_{2,j,m-1}$ during the integration of any single tracer pair, for inconsistencies with $\hat{\mu}_{i,j,m} > 1$ or < -1 can easily occur.

To determine the $\mu_{i,j,m-1}$ we define a parameter $G = [(r_{m-1})/r_m]$. It will be seen that the selection of a value for G is the equivalent of the selection of a time step. This definition is motivated in Appendix C where it is shown how the $\mu_{i,j,m-1}$ can be accurately determined by using $G\boldsymbol{r}_m$ in (21) in place of $\boldsymbol{r}_m$. An important part of this development is that G, selected to be slightly less than 1, determines the variable time step by

$$\Delta t_m = F(1-G)r_m^{1-\beta}/(GC_1). \tag{26}$$

By this definition of G the time step increases with r such that the ratio $(r_{m-1})/r_m$ remains statistically constant even though r increases by several orders of magnitude. The factor F ideally should be 1.0, but the value used in the final computations was precisely chosen by trial to satisfy the condition that the calculated value $[(r_{m-1})/r_m]$ equals the chosen value of G. A range of values of G was tested and for $G > 0.92$ there were no essential differences in the results, but $G = 0.96$ was used in the final computations to assure accuracy, and for this G the above condition gave $F = 1.01$.

(*b*) The objective is: given a set of six correlations $\hat{\mu}_{i,j} = \overline{\hat{u}_{1,i}\hat{u}_{2,j}}$ from (25) at each time step, find six random values, $\hat{u}_{1,i}$ and $\hat{u}_{2,j}$, such that if the procedure were applied many times starting with the same $\hat{\mu}_{i,j}$ the sets of $\hat{u}$ would satisfy these correlations. The constraints

$$\overline{\hat{u}_{1,i}u_{1,j}} = \delta_{i,j}, \quad \overline{\hat{u}_{2,i}\hat{u}_{2,j}} = \delta_{i,j} \tag{27}$$

also must be met to satisfy the condition that orthogonal components at the same point are not correlated and that the $\hat{u}$ have zero means and unit variances.

The $\hat{u}_{1,i}$ are chosen first randomly and independently from a normal distribution together with three additional random numbers, $\hat{s}_1$, $\hat{s}_4$, and $\hat{s}_5$. The algorithm for then finding the $\hat{u}_{2,j}$ is tedious and is relegated to Appendix D. There is no bias introduced by selecting the $\hat{u}_{1,i}$ first because the $\hat{u}_{2,j}$ so determined also have normal distributions and are independent of each other. (In comparative calculations the $\hat{u}_{1,i}$ and the $\hat{u}_{2,j}$ were chosen first alternately and this demonstrated no difference in the statistical results.)

6. The numerical model

6.1. *Major sections of the computer program*

(*a*) Initialization. For each tracer pair the initial component spacings $r_{i,o}$ were randomly selected from a Gaussian distribution with a standard deviation of 10^{-10}. The resultant r_o was then the basis for calculating the required initial relations $\mu_{i,j,o} = \overline{u_{1,i,o}\, u_{2,j,o}}$ from (21) and the individual values of $u_{1,i,o}$ and $u_{2,j,o}$ were found using the algorithm of Appendix D. These values, however, if found for many cases with the same $\mu_{i,j,o}$ would not generally satisfy all of the moments of $u_{1,i}$ and $u_{2,j}$ that are found during a time integration of the equations. Thus, transient adjustments should be expected due to this imperfect initialization. In this study the adjustment time of $t = 10^{-5}$ (approximately 250 time steps) was found to be adequate to obtain stable values of C_1 and C_2 as well as stable third and fourth moments of U.

Other tests of the initial conditions confirmed that fixing either r_o or the $u_{1,i,o}$ for all tracer pairs did not affect the statistical results, as should be expected, but correct computation of the initial coorelations by the method of Appendix D was essential to avoid very long transients.

(*b*) At each time step and for each tracer pair:

(i) Δt_m for the spacing r_m was found from (26), and new values of R_m and Q_m were computed.

(ii) The $\mu_{i,j,m}$ and $\mu_{i,j,m-1}$ based upon r_m and Gr_m, respectively, were calculated, and the $\hat{\mu}_{i,j,m}$ were found from (25).

(iii) The $\hat{u}_{1,i,m}$ were randomly selected and the $\hat{u}_{2,j,m}$ were found by the algorithm of Appendix D.

(iv) The six $\hat{u}$ from (iii) were used in (9) and (10) to find new velocity components $u_{1,i,m}$ and $u_{2,j,m}$, the differential speeds $U_{i,m}$, and then new spacings $r_{i,m+1}$.

Appendix E provides the complete sequence of equations solved at each time step.

(v) Special analyses of the data were required at selected times. As examples: (I) To compute the autocorrelation of velocities, the U_i at each step were scaled to correspond to a fixed length and, therefore, a fixed time step. (II) To obtain the distribution functions at fixed times and other summaries, data were accumulated at 16 logarithmically equally spaced fixed times from $t_f = 10^{-5}$ to 1.5×10^{-3}. When a calculation passed any t_f, for data summaries the r and r_i were interpolated to that time level. (III) At these same times the U were scaled (see below) for the calculation of C_1 and C_2.

(*c*) As necessary several 'runs', each with N pair, were carried out to obtain estimates of the uncertainty of the statistical results. Usually $N > 1000$.

6.2. *Computation of the output values $C_{1,o}$ and $C_{2,o}$*

For each run output values $C_{1,o}$ and $C_{2,o}$ were found from

$$C_{1,o} = [U/r^{\beta}], \quad C_{2,o}^2 = [U^2/r^{2\beta}]. \tag{28}$$

These formulae deserve special comment because they differ from (3) and (4) and because one can easily obtain biased results from wrong selection of the data to be averaged.

To evaluate C_1 and C_2 from (3) and (4) one should find averages $\langle U \rangle$ and $\langle U^2 \rangle$ at some fixed r_f. One plan might be to select an r_f and as each tracer crossed r_f, either with $U > 0$ or $U < 0$, to record and average U and U^2. The error of such a method would be clear when the distribution of U was examined, for there would be no events at $U = 0$. Clearly, there is a bias according to the value of U itself. This pitfall can be avoided by selecting values of U at some fixed time, t_f. Then if both r and U for many pairs are recorded at t_f and the values are sorted into N ($n = 1-N$) bins with widths Δr and average lengths r_n, the values of U at each r_n can be used to calculate $\langle U \rangle (r_n)$ and $\langle U^2 \rangle (r_n)$. In addition, values from several t_f could be combined.

But a more efficient method that avoids the sorting of U and U^2 according to r uses the knowledge that in the inertial subrange C_1 and C_2 are independent of r. If each $U(r)$ is divided by r^{β} and each U^2 by $r^{2\beta}$ this is the equivalent of finding individual estimates $C_1 = U/r^{\beta}$ and $C_2^2 = U^2/r^{2\beta}$. Equations (28) correspond to averages of these individual estimates, and data from various t_f and r can be combined. Then once suitable averages of C_1 and C_2 have been found, one can obtain $\langle U \rangle (r)$ and $\langle U^2 \rangle (r)$ from (3) and (4).

Two additional possible sources of bias should be mentioned. All integrations must be long enough for each tracer pair to pass all values of t_f. If, for example, some slowly separating pairs were cut short before passing the largest t_f, $C_{1,o}$ and $C_{2,o}^2$ would be biased toward large values. Moreover, bias will occur if the samples are taken at intervals of a fixed number of time steps because of the variable time step and its relation to r and U.

Ideally the t_f should be separated sufficiently to assure independent samples of U. In the present study sixteen t_f were used, but it will be seen from the autocorrelations of U that these were the equivalent of only two independent samples.

6.3. *Matching input and output values of C_1 and C_2, and the determination of F*

Input and output values of C_1 and C_2 had to be matched by trial and error for several values of G, Cs, and F to test their effects on C_1 and C_2. For each combination of G, Cs, and F about 30 cases were tried, each with 1000 tracer pairs and a different combination of inputs $C_{1,i}$ and $C_{2,i}$. For each case with $N = 1000$ there were about 2000 independent samples. For matching purposes the variates to be analysed were the ratios $C_{1,r} = C_{1,o}/C_{1,i}$ and $C_{2,r} = C_{2,o}/C_{2,i}$ with the goal of $C_{1,r} = C_{2,r} = 1$, simultaneously. For any one case the standard deviation of the means of $C_{1,r}$ and $C_{2,r}$ were typically ± 0.009 and ± 0.006, respectively.

For the approximately 30 cases the lines $C_{1,r}(C_{1,i}, C_{2,i}) = 1$ and $C_{2,r}(C_{1,i}, C_{2,i}) = 1$ were found by the method of least squares. Their intersection gave estimates of C_1 and C_2 where $C_{1,r} = C_{2,r} = 1$, and the acceptability of these C_1 and C_2 were checked by further computation to assure consistent values.

The ratio $G_r = [(r_{m-1})/r_m]/G$ should be unity according to the definition of G, and the condition $G_r = 1$ was the basis for the selection of a consistent value of F. Here again to avoid bias averages must be for data at fixed time levels, but the data from several time levels can be averaged.

6.4. *The computation of* C_0

For selected values of Cs and G and with consistent values of C_1, C_2 and F, C_0 was computed from (2) using values of r interpolated to the times, t_f. For any two time levels t_a and t_b, C_0 can be found from the integrated form of (2)

$$(r_b^+)^{(1-\beta)} - (r_a^+)^{(1-\beta)} = C_0(1-\beta)(t_b - t_a), \tag{29}$$

where r_b^+ and r_a^+ are the r.m.s. values of r for t_b and t_a. The use of 16 time levels allowed the calculation of 15 values of C_0 in each run and these were averaged.

7. Results

7.1. *The effects of G, Cs and the value of F*

Values of G above about 0.92 showed no significant differences in the results, but for the assurance of accuracy $G = 0.96$ was used for all of the final computations.

Consistent values of C_1 and C_2 for $F = 1$ were found at five values of Cs from 2.0 to 3.4. There were no trends of C_1 or C_2 with Cs, and it is concluded that the non-dimensional results are independent of Cs over the range indicated above. Dimensional results, however, will depend upon the value used for Cs.

Consistent values of $C_1(F)$, $C_2(F)$ and the ratio $G_r(F)$ were found for several values of F. By interpolation to $G_r(F) = 1$, the value $F = 1.01$ was determined to be correct at $G = 0.96$. Therefore $F = 1.01$ and the corresponding results $C_1(1.01) = 1.273$ and $C_2(1.01) = 1.581$ were applied to all further computations.

7.2. *Internal consistency of the calculations*

A correct evaluation of (25) is crucial to the success of this model. It would be desirable to directly compare calculated values of these sensitive correlations with theory for several fixed $\boldsymbol{r}$, but it is not practical to compute correlations for any specific vector. It is practical, however, to compare calculated and theoretical $\hat{\mu}_{i,j}$ averaged over all directions for fixed r.

The theoretical directionally averaged $\mu_{i,j,m}$ and $\mu_{i,j,m-1}$ in (25) are found by globally averaging (21). With $i = j$ the average of $r_i r_i / r^2$ is $1/3$. For $i \neq j$ the averages are 0. By theory $\langle 1 - \hat{\mu}_{i,i}(\text{th}) \rangle$ changes only from 0.0763 to 0.0769 over our range of r and the average value 0.0766 is drawn in figure 2. The averages $[1 - \hat{\mu}_{i,i}(\text{com})]$, found from the computed random numbers at fixed t_f, are shown in figure 2 with 50000 entries for $\hat{\mu}_{i,i}(\text{com})$ at each t_f. Despite the large fluctuations from the beginning, the average is 0.0701, very close to the theoretical value considering the scatter of the data, and there is no obvious trend with time. This confirms that the model is internally consistent and that the calculations are accurate. The large fluctuations seen at small t_f in figure 2 appear to be a computer round-off problem in the calculation of $\mu_{i,i}(\text{com})$, and no other statistics have exhibited similar fluctuations.

7.3. *The values of* C_1, C_2 *and* C_0

With $Cs = 3$, $G = 0.96$ and $F = 1.01$, the consistent values $C_1 = 1.273$, $C_2 = 1.581$ were found. With these as input the average C_0 found from 20 runs, each with 2000 tracer pairs, was $C_0 = 1.459 \pm 0.002$. Table 1 is an example of statistics from the first of those 20 runs.

It may be seen from (18) and (19) that for $C_1 = 0$ and $C_2 = 2$ the Kármán/Howarth relations are retrieved. Using the same program but with these values, i.e. with the Eulerian relations, the expansion constant was found to be $C_{0,E} = 1.780 \pm 0.004$.

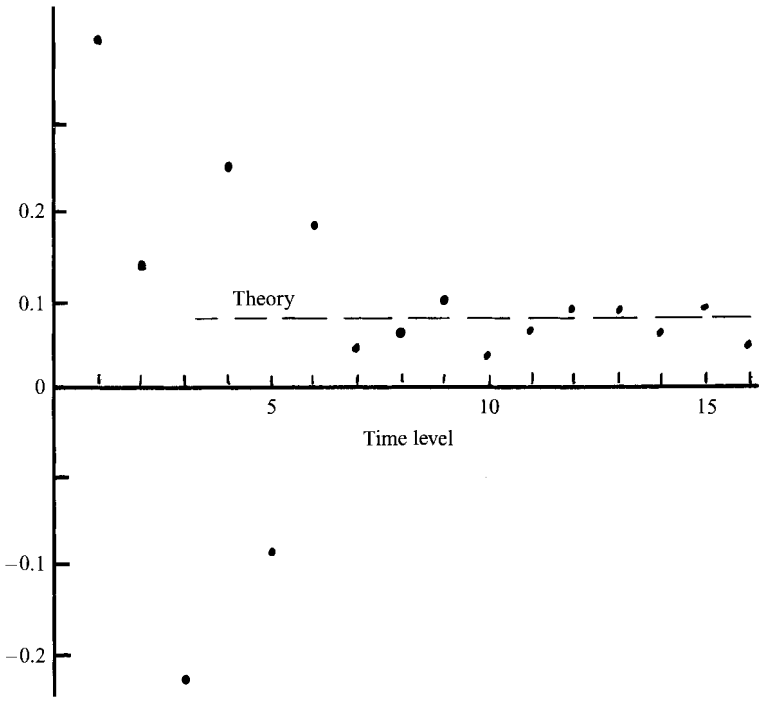

FIGURE 2. Computations of the directionally averaged right-hand side of (25) for comparison with theory. Plotted point are computations of $[1-\hat{\mu}_{i,j}(\text{com})]$ for 50000 tracer pairs at the 16 time levels. The dashed line is the theoretical average value $[1-\hat{\mu}_{i,j}(\text{th})] = 0.0766$.

Time level	$\ln(t_f)$	$\ln(r^+)$	C_0	$K(r)$	$K(r_i)$
2	−11.18	−16.78	1.450	2.323	4.144
3	−10.84	−16.29	1.448	2.350	4.216
4	−10.51	−15.79	1.455	2.349	4.237
5	−10.18	−15.30	1.444	2.325	4.197
6	−9.843	−14.81	1.436	2.359	4.197
7	−9.508	−14.31	1.440	2.372	4.186
8	−9.175	−13.71	1.443	2.334	4.116
9	−8.941	−13.32	1.439	2.269	4.009
10	−8.506	−12.82	1.428	2.244	3.988
11	−8.173	−12.32	1.440	2.284	4.108
12	−7.839	−11.81	1.455	2.315	4.181
13	−7.504	−11.30	1.504	2.353	4.228
14	−7.170	−10.78	1.506	2.357	4.227
15	−6.836	−10.28	1.482	2.305	4.166
16	−6.502	−9.780	1.469	2.279	4.095

TABLE 1. Some statistical results at time level $t_f = 2$–16. The first of 20 runs with $N = 2000$ from which final averages of C_0 and K were computed. $K(r)$ and $K(r_i)$ are the kurtoses of r and r_i, respectively. Slow oscillations in C_0 and the K reflect the autocorrelation of U and the fact that data at the 16 t_f correspond to only two independent samples.

Figure 3 illustrates five typical trajectories of $\ln(r)$ *vs.* $\ln(t)$ with dots every five time steps. The slopes of these trajectories may be compared to the theoretical average slope $1/(1-\beta) = 1.50$. Approximately 30% of the time $U < 0$. The trajectories also give an impression of the autocorrelation time of the separation speed, U.

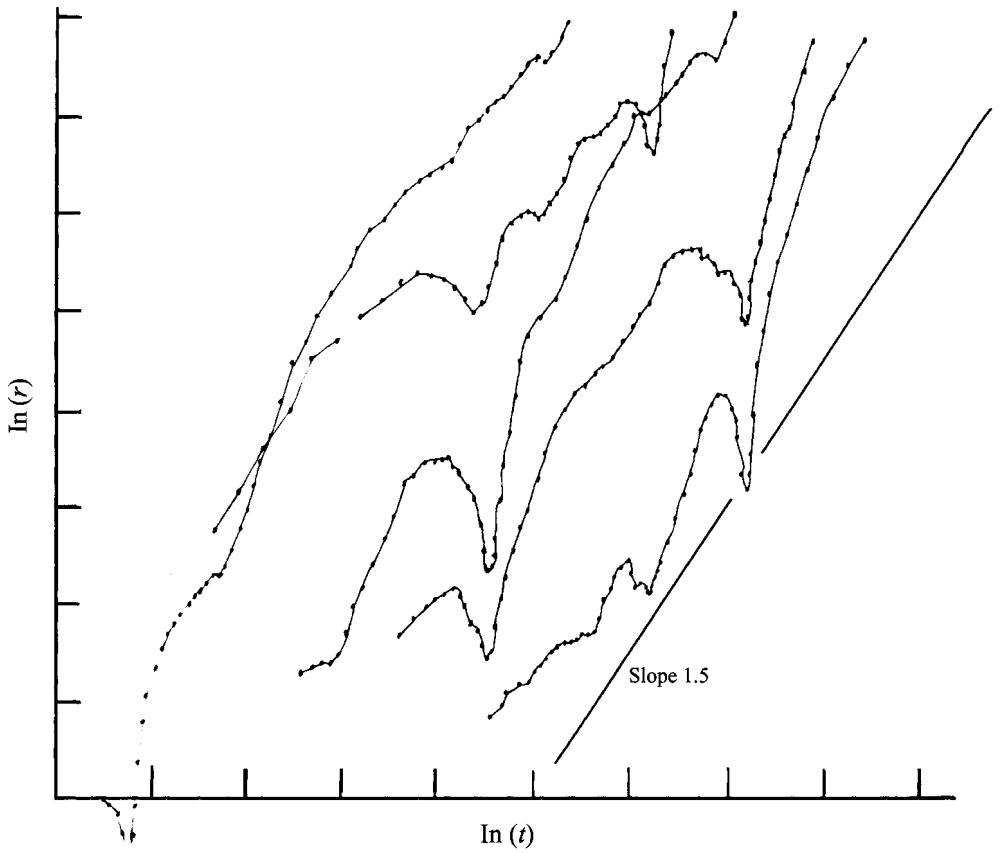

FIGURE 3. Five examples of trajectories of $\ln(r)$ *vs.* $\ln(t)$. Plotted points are at every five time steps. Successive curves are displaced by one unit to the right. The straight line is the theoretical slope, $1/(1-\beta) = 3/2$.

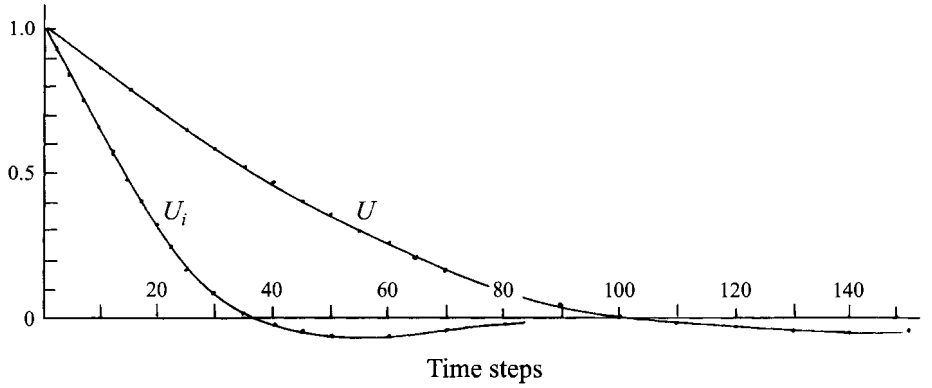

FIGURE 4. Autocorrelation curves for U and U_i as a function of the number of time steps with $G = 0.96$. Plotted points are at 5-time-step lags. The curves fall to 1/e at 98 and 37 time steps for U and U_i, respectively.

7.4. *Autocorrelations of U and of its components, U_i*

Figure 4 illustrates the autocorrelations of U and U_i as functions of the number of time steps at $G = 0.96$. To obtain a time series suitable for autocorrelation, U and U_i at length r were scaled to a fixed length by $(r_f/r)^\beta$ so that there would be no trends in

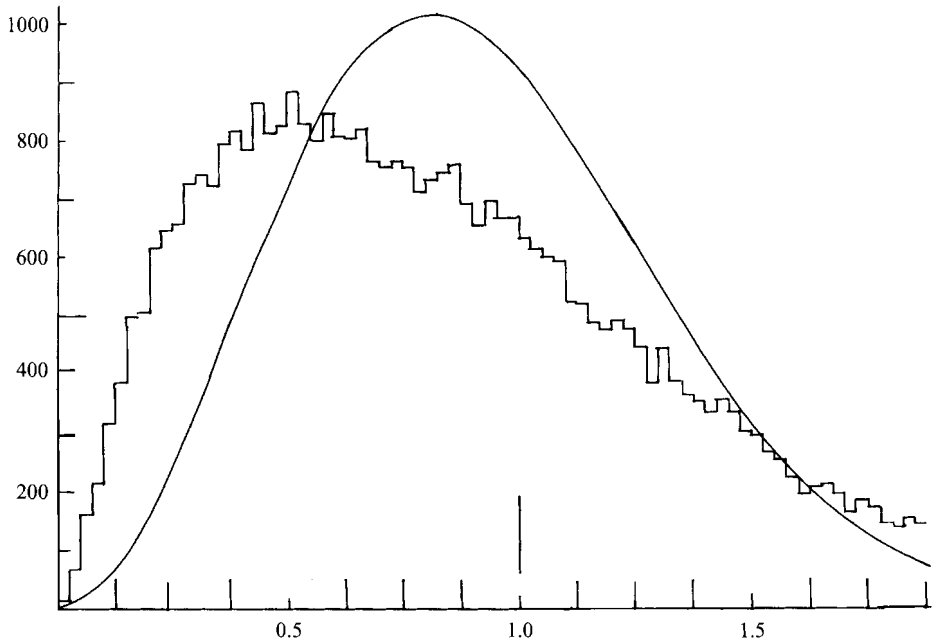

FIGURE 5. A histogram of r at fixed t. The curve is the three-dimensional Gaussian with the same area and variance as the histogram. The large line from the abscissa is one standard-deviation about the origin. The histogram is found from 40000 values of r.

the velocities and so that the time step represented by each U would be the same. The number of steps at which the two curves reach 1/e are 37 for U_i and 98 for U, and these are taken to be estimates of the integral scales of the two curves.

The number of steps between the t_f time levels used for data analysis averaged only 15, so it is clear that data at the 16 t_f were not all independent. Requiring two integral scales for independent data, it seems that for each tracer pair U had only two independent values. This conclusion is borne out by the trajectories of figure 3 and by the examination of other data. For example, the values of C_0 and K in table 1 show slow oscillations of these statistics with timescales comparable to the integral scale of U.

Figure 4 also shows that for $G = 0.96$ the time step is short compared to the integral scale of U_i thus assuring computational accuracy in this respect. These integral scales also can be guides for direct observations of relative tracer motions or for the analysis of computer simulations. This point will be considered further in §8 where examples of the conversion to dimensional variates are given.

7.5. *The distributions of r and r_i*

The distribution of r at a fixed time is given in figure 5 where the histogram shows the calculated distribution and the curve gives the three-dimensional Gaussian distribution that has the same area and variance as the histogram. Moments of these distributions are taken about the origin because mirror-image curves should occur for $r < 0$. The kurtosis of the three-dimensional Gaussian is $K = 1.667$ and that of the histogram is $K = 2.285 \pm 0.010$ standard mean deviation, somewhat larger because at large r many histogram values exceed those of the Gaussian. The excess at small r is detailed in figure 6 where it may be seen that the frequency is 6 to 10 times that of the Gaussian. The histogram of figure 6 is well fit by a straight line over a range of r but this line does not

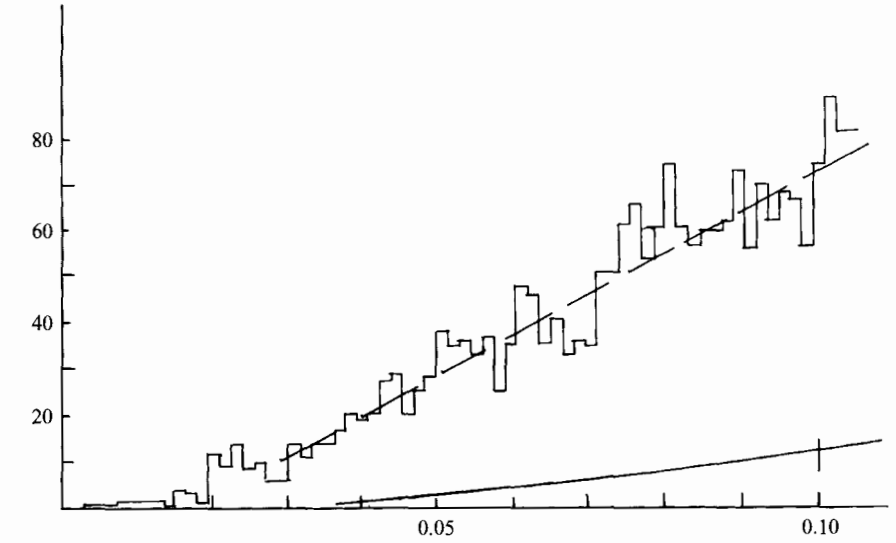

FIGURE 6. The same as figure 5 but for r close to the origin. Only 2355 of the 200000 total values of r fell into this range, $0 < r < 0.105$. As in figure 5 the abscissa scale is in terms of the standard deviation of the Gaussian.

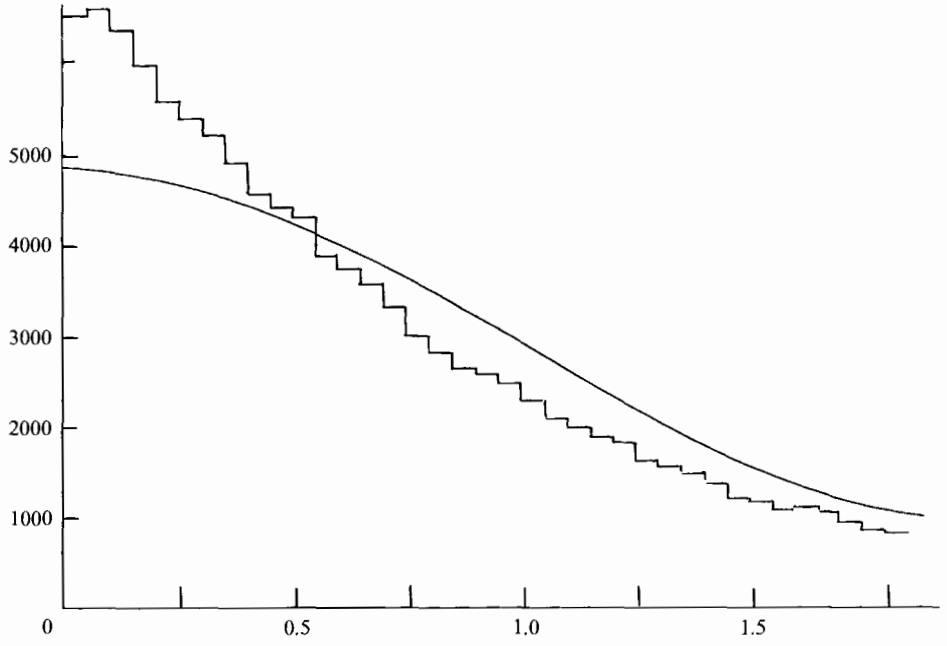

FIGURE 7. A histogram of the components r_i for 120000 values and the corresponding Gaussian curve. Negative values of r_i have been rectified because of symmetry. The abscissa is in terms of the standard deviation of the two curves. The histogram exceeds the curve at larger r_i.

intersect the origin. Further extensive calculations confirmed that the curve is parabolic very close to $r = 0$.

Figure 7 gives a histogram of the components r_i in comparison with a Gaussian. The histogram kurtosis is $K_i = 4.119 \pm 0.017$ standard mean deviation compared to $K = 3$ for the Gaussian. The larger K_i indicates that the histogram is more peaked than the

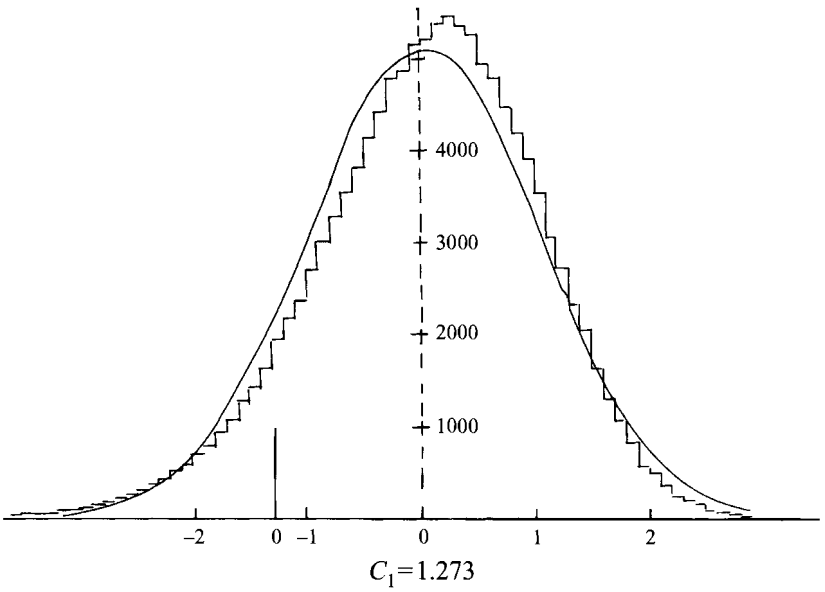

FIGURE 8. A histogram of the separation speed U for 224000 values and the comparable Gaussian curve. The tall line on the abscissa is $U = 0$. Shorter lines are at 1 and 2 standard deviations from the mean (dashed line). These data for U have a negative skewness similar to that for the Eulerian U^*.

corresponding Gaussian. The data for $K(r)$ and $K(r_i)$ in table 1 show that to fourth order the distributions show no trend, only small oscillations, thoughout the computations.

7.6. *The distribution of U at fixed r*

Figure 8 gives a histogram of U/r^{β} in comparison with the corresponding Gaussian, and for fixed r this histogram is also the distribution of U. The mean has the value of C_1. This histogram has skewness $Sk = -0.45$, negative as in the distribution of U^* (Anselmet *et al.* 1984). The corresponding distribution of the U_i indicates only a slight but systematic departure from Gaussian.

8. Conclusions

This new random-flight model for relative dispersion in idealized turbulence evaluates and uses the two previously undetermined constants defined in Faller (1992). The consistent values $C_1 = 1.273$ and $C_2 = 1.581$ have been determined by a trial and error procedure. The model satisfies all the second-order two-tracer Lagrangian velocity relations, similar to those for the Eulerian Kármán/Howarth correlations. Although these Lagrangian relations are purely kinematic constraints, it is believed that the random-flight equations, coupled with these constraints, produce a fair model of relative dispersion. Dynamics enters the model by specification of the turbulent intensity and the Lagrangian integral timescale.

The average of many values of $\hat{\mu}_{i,j}$ as found from (25) has shown good agreement with theory. Many other checks of computed statistics, for example verification that $[s_2^2] = [s_3^2] = 1$ and $[u_{2,1}^2] = [u_{2,2}^2] = [u_{2,3}^2] = 1$, have shown that the model is internally consistent and that the computational program is correct and accurate. Table 1 shows that the statistics are stable over the length of time for which results were recorded aside from small stochastic fluctuations.

The Lagrangian value of the expansion coefficient is $C_0 = 1.459$. (Note that r is the spacing of tracers, not the cloud radius. The expansion coefficient for the r.m.s. radius of a cloud, $(\tilde{\rho}^2)^{\frac{1}{2}}$, is $C_0/1.414 = 1.032$.) This is substantially less than $C_{0,E} = 1.78$, found when the Eulerian correlations are used. The significance of this difference is clear in the Richardson t^3 law, which in non-dimensional form is

$$r^{+2} = \gamma \epsilon^{1/3} t^3, \tag{30}$$

where γ is an undetermined constant $O(1)$ and ϵ is the non-dimensional dissipation rate. Then from an integration of (2) it is readily found for large t that

$$r^{+2} = (2C_0/3)^3 t^3; \tag{31}$$

hence $\gamma = (2C_0/3)^3 \epsilon^{-1}$. Comparing the Lagrangian and Eulerian values of γ the ratio is

$$\gamma_L/\gamma_E = (C_0/C_{0,E})^3 = 0.55. \tag{32}$$

Some examples of a conversion to dimensional quantities may be useful. Dimensional variates for time, length, and speed are found from

$$t' = CsTt = Lt/u', \quad r' = rL, \quad \text{and} \quad U' = Uu'.$$

In a laboratory situation take $L = 100$ cm and $u' = 5$ cm s^{-1}, and suppose measurements at a spacing of $r' = 1$ cm. From this model with $G = 0.96$ and at $r = 0.01$ the time step would be $\Delta t = 0.001\,53$ and $\Delta t'$ would be 0.0306 s. Since the correlation time of U_i is 37 Δt for $G = 0.96$, the correlation time of a dimensional component U_i' would be 1.13 s, and the correlation time of U' would be 2.6 s. Thus, observations would have to be separated by at least 5 s to have reasonably independent samples of U' from the same pair of tracers.

For an atmospheric example take $L = 1000$ m and $u' = 5$ m s^{-1} and take a particle pair with a separation of 1 m. The correlation time for a component U_i' would then be 2.4 s and that of U' would be 6.7 s. Thus $\Delta t' \ll 2.4$ s would be required to adequately simulate two-particle dispersion computationally for the specified conditions.

The distribution of r shows distinctly non-Gaussian characteristics with a more peaked distribution. Figures 5 and 6 imply much greater concentrations of tracers or pollutants at small r than would be expected from an equivalent Gaussian cloud.

Finally, it is interesting to compare the skewness of U as seen in figure 8 with that for the parallel velocity difference at two fixed points, U^*. The model skewness is $Sk = -0.45$. The theoretical skewness for U^* from Monin & Yaglom (1971) can be written as $Sk = -0.283b$ (see Faller 1992, Appendix E) where the dissipation rate has been written as $\epsilon' = bu'^3/L$. If b were 1.63 these skewness values would be the same.

The characteristics of relative dispersion considered here eventually will be determined by direct numerical solution of the Navier–Stokes equations. In the meantime numerical models do not reach sufficiently high Reynolds numbers and observations are not adequate for definitive results. This model provides a guide for future studies, and the method, with variations, may prove to be useful in a variety of dispersion problems.

This research was supported in part by past grants from the National Science Foundation: ATM 3217139 and MSM 8617897. Special thanks are extended to Mr Gi-Sang Choi who assisted with the early phases of this study as a graduate student at the University of Maryland.

Appendix A. The relations between S, α and β

A.1. *The relation of β to S*

We may hypothesize a subrange with a slope S and the flux of some quantity through this subrange at rate Ω'. For the traditional cases of $S=-5/3$ in two or three dimensions, Ω' would the flux of energy, ϵ'; and for $S=-3$ in two-dimensional turbulence Ω' would be the flux of enstrophy, η'.

For the three-dimensional subrange dimensional arguments give

$$\mathrm{d}(r^+)^2/\mathrm{d}t = D_1(\epsilon)^{1/3}(r^+)^{4/3}, \tag{A 1}$$

where D_1 is a non-dimensional constant $O(1)$ and ϵ is dimensionless. But from (2) we may also write

$$\mathrm{d}(r^+)^2/\mathrm{d}t = 2C_0^2(r^+)^{(1+\beta)} \tag{A 2}$$

and it is apparent that $\beta = 1/3$ and $2C_0 = D_1(\epsilon)^{1/3}$.

For the two-dimensional enstrophy cascade it is similarly found that $\beta = 1$ and $2C_0 = D_2(\eta)^{1/3}$. Thus for $S=-5/3$, $\beta = 1/3$ and for $S=-3$, $\beta = 1$, and the relation

$$\beta = -(S+1)/2 \tag{A 3}$$

is suggested. From similar arguments for an arbitrary (within limits) S, relation (A 3) applies if the dimensions of Ω' are such that it enters an equation like (A 1) to the 1/3 power.

A.2. *The relation of α to β and to S*

We begin with the identity

$$\langle U^{*2}\rangle \langle U\rangle^2/\langle U^{*2}\rangle = \langle U\rangle^2. \tag{A 4}$$

Expanding the left-hand side by

$$\langle U^{*2}\rangle = \langle (u^*_{2,p} - u^*_{1,p})^2\rangle = 2u^2(1-f^*), \tag{A 5}$$

where

$$f^* = \langle u^*_{2,p} u^*_{1,p}\rangle/u^2 = \exp(-r^\alpha) \sim 1-r^\alpha, \quad \text{and} \quad u^2 = 1,$$

and expanding the right-hand side using (3), it follows that

$$2r^\alpha \langle U\rangle^2/\langle U^{*2}\rangle = C_1^2 r^{2\beta}. \tag{A 6}$$

But because both C_1^2 and $\langle U\rangle^2/\langle U^{*2}\rangle$ must be independent of r, it follows quite generally that $\alpha = 2\beta$. Moreover, for the familiar examples of $S=-5/3$ and $S=-3$ the relation

$$\alpha = -(S+1) \tag{A 7}$$

is valid, and (A 7) applies more generally to the extent that (A 3) is applicable.

Appendix B. Additional relations involving $u_{1,p}$, $u_{2,p}$, $u_{1,n}$ and $u_{2,n}$

The formula for $\langle u^2_{1,p}\rangle$ may be found in Faller (1992) and is

$$\langle u^2_{1,p}\rangle = \langle u^2_{2,p}\rangle = (1+f^*)/2 + \langle U^2\rangle/4. \tag{B 1}$$

In the inertial subrange and expanding $f^* = 1-r^\alpha$ we can write (B 1) as

$$\langle u^2_{1,p}\rangle = 1 - r^\alpha/2 + C_2^2 r^\alpha/4. \tag{B 2}$$

Thus the Lagrangian case reduces to the Eulerian $\langle u^2_{1,p}\rangle^* = 1$ if $C_2^2 = 2$, and of course in the Eulerian case $C_1 = 0$.

For one of the two normal components at point 1, with $u_{1,n}$ taken in an arbitrary normal direction, note that

$$\langle u_{1,1}^2+u_{1,2}^2+u_{1,3}^2\rangle = 3 = \langle u_{1,p}^2\rangle+2\langle u_{1,n}^2\rangle; \tag{B 3}$$

hence for this one normal component

$$\langle u_{1,n}^2\rangle = \langle u_{2,n}^2\rangle = (3-\langle u_{1,p}^2\rangle)/2. \tag{B 4}$$

Then with $\langle u_{1,n}\rangle = \langle u_{2,n}\rangle = 0$ it is apparent that $\sigma(u_{1,n}) = \sigma(u_{2,n}) \neq 1$, and, as noted in §4, $g = \langle u_{1,n}u_{2,n}\rangle$ is a covariance but not a proper correlation coefficient.

Equations (B 1) and (B 2) can be used to find the true correlation coefficients $\mathrm{Cor}\,(u_{1,p}u_{2,p})$ and $\mathrm{Cor}\,(u_{1,n}u_{2,n})$ in terms of C_1 and C_2 when (3) and (4) are applied. These correlations reduce to f^* and g^* for $C_1 = 0$ and $C_2^2 = 2$.

Appendix C. The determination of Δt_m and the $\mu_{i,j,m-1}$

C.1. *Formulation of a variable time step*

Consider the backward-time-step finite-difference approximation of (3), averaged for many cases that led to a specific r_m, namely

$$(r_m-\langle r_{m-1}\rangle)/\Delta t_m = C_1 r_m^{\beta}, \tag{C 1}$$

where $\langle r_{m-1}\rangle$ is an E2-average of the lengths r_{m-1} for the fixed r_m. From the definition $G = [(r_{m-1})/r_m]$, for a specific r_m, $\langle r_{m-1}\rangle = Gr_m$ and (C 1) becomes

$$\Delta t_m = (1-G)\,r_m^{1-\beta}/C_1 \tag{C 2}$$

as a temporary definition of a variable Δt_m in terms of the constant G. Note that

$$(1-G) = (r_m-\langle r_{m-1}\rangle/r_m$$

is the fractional change of r, statistically, in one time step. Thus a fixed G provides a variable Δt_m such that the fractional change of r is constant as r increases over several orders of magnitude.

The backward step in (C 2) was used to provide a specific definition for G that is used in §C 2 below. To convert (C 2) to a forward time step one need only divide by G. To obtain the formula used in the computations a factor F also has been added to give

$$\Delta t_m = F(1-G)\,r_m^{1-\beta}/C_1 G. \tag{C 3}$$

F was introduced to compensate for small errors due to the finite time step and should be close to 1. For $G = 0.96$ the consistent value, as explained in §7, was found to be $F = 1.01$.

C.2. *Evaluation of the* $\mu_{i,j,m-1}$

The individual values r_{m-1} in (B 1) are the magnitudes of vectors $\boldsymbol{r}_{m-1}$ that may be thought of as follows: for N integrations that may have by chance led to the same $\boldsymbol{r}_m$ there would have been N different vectors $\boldsymbol{r}_{m-1,n}, n = 1-N$. For large N an average vector, $\boldsymbol{r}_{m-1}^a$ would lie along the direction of $\boldsymbol{r}_m$ with a magnitude r_{m-1}^a, as illustrated in figure 9. If the N vectors at $m-1$ do not vary much in direction, the average magnitude $\langle r_{m-1}\rangle$ will be nearly the same as r_{m-1}^a and we may write that approximately $\boldsymbol{r}_{m-1}^a = G\boldsymbol{r}_m$.

For each $\boldsymbol{r}_{m-1,n}$ there are corresponding products $(u_{1,i}u_{2,j})_{m-1,n}$. Averages of these products for each combination of i and j and for large N are the desired $\mu_{i,j,m-1}$. Again, if the individual $\boldsymbol{r}_{m-1,n}$ are not too different one may expect that estimates of $\mu_{i,j,m-1}$ found from the average vector $\boldsymbol{r}_{m-1}^a = G\boldsymbol{r}_m$ should be good approximations to the true

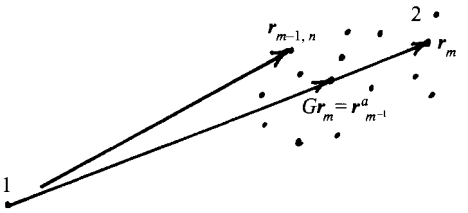

FIGURE 9. An illustration of a vector r_m and hypothetical vectors $r_{m-1,n}$ plotted so that points 1 coincide. The cloud of terminal points 2 has a centroid that defines the terminus of a vector Gr_m that is used to determine the $\mu_{i,j,m-1}$.

values. In tests it has been found that for $G = 0.96$ the vectors r_{m-1} differ in direction from r_m with a standard deviation of only 2 degrees, so we may expect that the use of Gr_m in (21) will give good estimates of $\mu_{i,j,m-1}$.

A comparison has been made between computed values of $\mu_{i,j,m-1}$ and theoretical values in the following way. For a fixed r_m theoretical values were found from (21) using the vector Gr_m. To obtain comparable values from the computational model, many ($N = 120000$) single forward steps were made, each starting from the same r_m to obtain many $r_{m+1,n}$. Each pair of vectors was then separately rotated and scaled back to make each of the $r_{m+1,n}$ identical with the original r_m, and these were thereafter called the r_m. The old fixed r_m then became the new and variable $r_{m-1,n}$. The variable initial velocity components $u_{1,i,m}$ and $u_{2,j,m}$ also were rotated and scaled to become the new $u_{1,i,m-1}$ and $u_{2,j,m-1}$. The resultant values

$$\mu_{i,j,m-1} = [\overline{(u_{1,i,m-1}\, u_{2,j,m-1})}]$$

were found to be indistinguishable from the theoretical values as far as the required accuracy in (25) was concerned. These comparisons were made at several orientations of r_m to test for any possible dependence upon angle. Thus the use of Gr_m for the determination of $\mu_{i,j,m-1}$ appears to be justified.

Appendix D. The generation of correlated velocity components

The following algorithm is applied to the determination of correlated initial velocity components $u_{1,i,o}$ and $u_{2,j,o}$ and correlated random components $\hat{u}_{1,i}$ and $\hat{u}_{2,j}$ at each time step. In this Appendix the derivation is written for the random components.

Given the six correlations $\overline{\hat{u}_{1,i}\hat{u}_{2,j}}$ we start by drawing six independent random values, $\hat{u}_{1,i}$, $\hat{s}_1$, $\hat{s}_4$ and $\hat{s}_5$ from a normal distribution. The three $\hat{u}_{1,i}$ and $\hat{s}_1$ are to be used directly while $\hat{s}_4$ and $\hat{s}_5$ are to be used to find correlated random numbers $\hat{s}_2$ and $\hat{s}_3$ which in turn are needed to find the $\hat{u}_{2,j}$.

The $\hat{u}_{2,j}$ are generated from

$$\hat{u}_{2,j} = \hat{\mu}_{i,j}\hat{u}_{1,i} + d_j\hat{s}_j \quad (i,j = 1\text{–}3, \text{ sum on } i \text{ only}). \tag{D 1}$$

The following comments on this formulation may be helpful.

(i) If the velocity components for $i = 1, 2, 3$ are referred to as $\hat{u}, \hat{v}, \hat{w}$, and the axes are x, y and z, an example of (D 1) for $j = 2$ is

$$\hat{v}_2 = \hat{\mu}_{x,y}\hat{u}_1 + \hat{\mu}_{y,y}\hat{v}_1 + \hat{\mu}_{z,y}\hat{w}_1 + d_2\hat{s}_2. \tag{D 2}$$

(ii) The fact that the $\hat{\mu}_{i,j}$ are appropriate coefficients for the expansion in (D 1) may be seen by multiplying (D 2) by $\hat{u}_1$ and averaging, noting that $\overline{\hat{u}_1^2} = 1$ while $\overline{\hat{u}_1\hat{v}_1} = \overline{\hat{u}_1\hat{w}_1} = \overline{\hat{u}_1\hat{s}_1} = 0$, leaving the identity $\overline{\hat{u}_1\hat{v}_2} = \hat{\mu}_{x,y}$.

(iii) It will be shown that $\hat{s}_2$ and $\hat{s}_3$ (to be found as functions of $\hat{s}_1$, $\hat{s}_4$, and $\hat{s}_5$) are independent of the $\hat{u}_{1,i}$, as is $\hat{s}_1$. This independence is needed in the derivations that follow.

(iv) The d_j will be determined as functions of the $\hat{\mu}_{i,j}$.

Squaring (D 1), i.e. multiplying (D 1) by

$$\hat{u}_{2,k} = \hat{\mu}_{i,k}\hat{u}_{1,i} + d_k \hat{s}_k \tag{D 3}$$

and E3-averaging leads to

$$\overline{\hat{u}_{2,j}\hat{u}_{2,k}} = \hat{\mu}_{i,j}\hat{\mu}_{i,k} + d_j d_k \overline{\hat{s}_j \hat{s}_k} \quad \text{(sum over } i\text{)}. \tag{D 4}$$

For $k = j$ (D 4) reduces to

$$1 = \hat{\mu}_{i,j}\hat{\mu}_{i,j} + d_j^2, \tag{D 5}$$

and thus

$$d_j = \pm(1 - \hat{\mu}_{i,j}\hat{\mu}_{i,j})^{1/2}, \tag{D 6}$$

where either root is acceptable because the d_j multiply the normally distributed random numbers, $\hat{s}_j$. Thus for $j = 2$, for example,

$$d_2 = \pm(1 - \hat{\mu}_{1,2}^2 - \hat{\mu}_{2,2}^2 - \hat{\mu}_{3,2}^2)^{1/2}. \tag{D 7}$$

For $k \neq j$ $\overline{\hat{u}_{2,j}\hat{u}_{2,k}} = 0$ and (D 4) reduces to

$$\overline{\hat{s}_j \hat{s}_k} = \hat{\mu}_{i,j}\hat{\mu}_{i,k}/d_j d_k. \tag{D 8}$$

For $j = 2$ and $k = 3$ an example of (D 8) is

$$\overline{\hat{s}_2 \hat{s}_3} = (\hat{\mu}_{1,2}\hat{\mu}_{1,3} + \hat{\mu}_{2,2}\hat{\mu}_{2,3} + \hat{\mu}_{3,2}\hat{\mu}_{3,3})/d_2 d_3. \tag{D 9}$$

Thus (D 8) gives three s-correlations: $\overline{\hat{s}_1 \hat{s}_2}$, $\overline{\hat{s}_2 \hat{s}_3}$, and $\overline{\hat{s}_3 \hat{s}_1}$, in terms of the known $\hat{\mu}_{i,j}$ and the known d_j.

Having already selected $\hat{s}_1$ we now use these $\hat{s}$ correlations to find $\hat{s}_2$ and $\hat{s}_3$. Here it may be noted that although $\hat{s}_1$, $\hat{s}_2$ and $\hat{s}_3$ are correlated they are random variates, but not independent random variates.

To find $\hat{s}_2$ let

$$\hat{s}_2 = h_1 \hat{s}_1 + h_2 \hat{s}_4. \tag{D 10}$$

Then it is apparent from the previous use of such formulae that $h_1 = \overline{\hat{s}_1 \hat{s}_2}$ and $h_2 = (1 - (\overline{\hat{s}_1 \hat{s}_2})^2)^{1/2}$, so $\hat{s}_2$ can be calculated from (D 10). Clearly $\hat{s}_2$ is a random variate with a normal distribution for it is the weighted sum of two normally distributed random variates, and because it has been calculated without reference to the $\hat{u}_{1,i}$ it is independent of the $\hat{u}_{1,i}$ as claimed above.

To determine $\hat{s}_3$ let

$$\hat{s}_3 = h_3 \hat{s}_1 + h_4 \hat{s}_2 + h_5 \hat{s}_5. \tag{D 11}$$

Then multiplying (D 11) in turn by $\hat{s}_1$ and then by $\hat{s}_2$ and averaging we find

$$\overline{\hat{s}_3 \hat{s}_1} = h_3 + h_4 h_1, \tag{D 12}$$

$$\overline{\hat{s}_2 \hat{s}_3} = h_3 h_1 + h_4, \tag{D 13}$$

which can be solved for h_3 and h_4. Finally, squaring (D 11) and averaging one finds

$$1 = h_3^2 + h_4^2 + h_5^2 + 2h_1 h_3 h_4 \tag{D 14}$$

from which h_5 can be found, and (D 11) can be used to find $\hat{s}_3$. Again, $\hat{s}_3$ is independent of the $\hat{u}_{1,i}$ since it depends upon only the $\hat{s}_1$, $\hat{s}_4$, and $\hat{s}_5$. This independence is necessary for the formation of (D 4) from (D 1) and (D 3). This completes the derivation of variates needed to calculate the $\hat{u}_{2,j}$ from (D 1).

Appendix E. The sequence of calculations

We are given Cs, F, G, α, β, C_1, and C_2. At the start of each time step we know r_m, $r_{i,m}$, $u_{1,i,m-1}$, and $u_{2,j,m-1}$ either from specified initial conditions or from a previous step. The equations to be solved are:

$$\Delta t_m = F(1-G)\, r_m^{\beta}/GC_1, \quad \text{from (26)}, \tag{E 1}$$

$$R_m = (2-Cs\,\Delta t_m)/(2+Cs\,\Delta t_m), \quad Q = (1-R^2)^{1/2} \quad \text{from (8)}, \tag{E 2}$$

$$\mu_{i,j,} = r_m^{2/3}(\tfrac{1}{6}+C_2^2/12-3C_1^2/4)\, r_{i,m}\, r_{j,m}/r_m^2 + (1+r^{2/3}(-2/3-C_2^2/3+3C_1^2/4))\,\delta_{i,j}, \quad \text{from (21)}, \tag{E 3}$$

$$\mu_{i,j,m-1} = \text{same as (E 3) but with } r_m \text{ replaced by } Gr_m \quad \text{and} \quad r_{i,m} \quad \text{by } Gr_i,m, \tag{E 4}$$

$$\hat{\mu}_{i,j,m} = (\mu_{i,j,m} - R_m^2\, \mu_{i,j,m-1})/(Q_m)^2, \quad \text{from (25)}. \tag{E 5}$$

Subscript m is now dropped up to (E 14).

$$d_j = +(1-\hat{\mu}_{i,j}\hat{\mu}_{i,j})^{1/2}, \quad \text{from (D 6)}, \tag{E 6}$$

$$\overline{\hat{s}_j \hat{s}_k} = \hat{\mu}_{i,j}\hat{\mu}_{i,k}/d_j d_k, \quad \text{from (D 8)}, \tag{E 7}$$

$$h_1 = \overline{\hat{s}_1 \hat{s}_2}, \quad h_2 = (1-h_1^2)^{1/2}, \quad \text{following (D 10)}, \tag{E 8}$$

$$\overline{\hat{s}_2 \hat{s}_3} = h_1 h_3 + h_4, \quad \text{from (D 13)}, \tag{E 9}$$

$$\overline{\hat{s}_3 \hat{s}_1} = h_3 + h_1 h_4, \quad \text{from (D 12)}, \tag{E 10}$$

Solve (E 10) and (E 11) for h_3 and h_4.

$$h_5 = (1-h_3^2-h_4^2-2h_1 h_3 h_4), \quad \text{from (D 14)} \tag{E 11}$$

Select six independent random numbers from a normal distribution $\hat{u}_{1,i}$, $\hat{s}_1$, $\hat{s}_4$ and $\hat{s}_5$:

$$\hat{s}_2 = h_1 \hat{s}_1 + h_2 \hat{s}_4, \quad \text{from (D 10)}, \tag{E 12}$$

$$\hat{s}_3 = h_3 \hat{s}_1 + h_4 \hat{s}_2 + h_5 \hat{s}_5, \quad \text{from (D 11)}, \tag{E 13}$$

$$\hat{u}_{2,j} = \hat{\mu}_{i,j}\hat{u}_{1,i} + d_j \hat{s}_j \quad \text{(sum only on } i\text{)}, \quad \text{from (D 1)}, \tag{E 14}$$

$$u_{1,i,m} = R_m\, u_{1,i,m-1} + Q_m\, \hat{u}_{1,i,m}, \quad \text{from (9)}, \tag{E 15}$$

$$u_{2,j,m} = R_m\, u_{2,j,m-1} + Q_m\, \hat{u}_{2,j,m}, \quad \text{from (10)}, \tag{E 16}$$

$$U_{i,m} = u_{2,i,m} - u_{1,i,m}, \quad U = (U_{i,m}\, U_{i,m})^{1/2}, \tag{E 17}$$

$$r_{i,m+1} = r_{i,m} + U_{i,m}\, \Delta t_m, \tag{E 18}$$

$$r_{m+1} = (r_{i,m+1}\, r_{i,m+1})^{1/2}. \tag{E 19}$$

Copies of the basic computer program written in Fortran for the Macintosh are available from the author upon request.

REFERENCES

ANSELMET, F., GAGNE, Y., HOPFINGER, E. J. & ANTONIA, R. A. 1984 High-order velocity structure functions in turbulent shear flows. *J. Fluid Mech.* **140**, 63–89.

BATCHELOR, G. K 1953 *The Theory of Homogeneous Turbulence*. Cambridge University Press.

BORGAS, M. S. & SAWFORD, B. L. 1994 A family of stochastic models for two-particle dispersion in isotropic homogeneous stationary turbulence. *J. Fluid Mech.* **279**, 69–99.

CORRSIN, S. 1963 Estimates of the relations between Eulerian and Lagrangian scales in large Reynolds number turbulence. *J. Atmos. Sci.* **20**, 115–119.

DICKEY, T. D. & MELLOR, G. L. 1979 The Kolmogoroff $r^{2/3}$ law. *Phys. Fluids* **22**, 1029–1032.

DOP, H. VAN & NIEUWSTADT, F. T. M. 1985 Random walk models for particle displacements in inhomogeneous, unsteady turbulent flows. *Phys. Fluids* **28**, 1639–1653.

DURBIN, P. A. 1980 A random-flight model of inhomogeneous turbulent dispersion. *Phys. Fluids* **23**, 2151–2153.

DURBIN, P. A. 1983 Stochastic differential equations and turbulent dispersion. *Natl Aero. & Space Admin.* Reference Publ. 1103.

FALLER, A. J. 1992 Approximate second-order two-point velocity relations for turbulent dispersion. *J. Fluid Mech.* **244**, 713–720.

FALLER, A. J & AUER, S. J. 1988 The role of Langmuir circulations in the dispersion of surface tracers. *J. Phys. Oceanogr.* **18**, 1108–1123.

FALLER, A. J. & CHOI, G.-S. 1985 Random-flight studies of relative dispersion in homogeneous and isotropic two- and three-dimensional turbulence. *Tech. Note* Bn-1035. Inst. for Phys. Sci. and Tech., Univ. of Maryland.

KÁRMÁN, T. VON & HOWARTH, L. 1938 On the statistical theory of isotropic turbulence. *Proc. R. Soc. Lond.* A **164**, 192–215.

MONIN, A. S. & YAGLOM, A. M. 1971 *Statistical Fluid Mechanics.* MIT Press.

RICHARDSON, L. F. 1926 Atmospheric diffusion shown on a distance-neighbour graph. *Proc. R. Soc. Lond.* A **110**, 709–737.

TAYLOR, G. I. 1921 Diffusion by continuous movements. *Proc. Lond. Math. Soc.* (2) **20**, 1196.

TENNEKES, H. & LUMLEY, J. S. 1972 *A First Course in Turbulence.* MIT Press.

THOMSON, D. J. 1986 A random walk model of dispersion in turbulent flows and its application to dispersion in a valley. *Q. J. R. Met. Soc.* **112**, 511–530.

THOMSON, D. J. 1987 Criteria for the selection of stochastic models of particle trajectories in turbulent flows. *J. Fluid Mech.* **180**, 529–556.

THOMSON, D. J. 1990 A stochastic model for the motion of particle pairs in isotropic high-Reynolds-number turbulence, and its application to the problem of concentration variance. *J. Fluid. Mech.* **210**, 113–153.